Fluorescent Peptide Biosensor for Probing CDK6 Kinase Activity in Lung Cancer Cell Extracts

Jessica Soamalala,[a] Sebastien Diot,[a] Morgan Pellerano,[a] Christophe Blanquart,[b] Mathieu Galibert,[c] Magali Jullian,[c] Karine Puget,[c] and May C. Morris*[a]

CDK6 kinase regulates cell-cycle progression in G1, together with CDK4, but has cell-, tissue- and developmentally distinct functions associated with transcription, angiogenesis and metabolism. Although CDK6 makes an attractive cancer biomarker and target, there are no means of assessing its activity in a complex environment. In this study, we describe the design, engineering and characterisation of a fluorescent peptide biosensor derived from 6-phosphofructokinase that reports on CDK6 kinase activity through sensitive changes in fluorescence intensity. This biosensor can report on CDK6 activity in a dose-dependent fashion, thereby enabling quantification of differences in kinase activity in complex and physiologically relevant environments. Further implementation of this biosensor in different lung and melanoma cell lines, as well as in mesothelioma cell lines derived from patients together with a CDK4 biosensor highlighted differences in kinase activity between CDK6 and CDK4 kinase. This work demonstrates the utility of these selective tools for monitoring two closely related kinases comparatively and simultaneously in the same samples, thereby offering attractive perspectives for diagnostic and therapeutic purposes.

Introduction

Cyclin-dependent kinase 6 (CDK6) was first identified in the early 1990s as a cyclin D binding partner and kinase involved in cell cycle progression.[1–5] CDK6 indeed plays a role in regulating progression through the G1 phase of the cell cycle by phosphorylating the Retinoblastoma tumour-suppressor protein p107Rb, like the closely related CDK4 kinase, thereby derepressing E2F and enabling transcription of genes required for progression into S-phase.[2–6] CDK6 was therefore long considered a redundant homologue of CDK4. Like the closely related CDK4 kinase, CDK6 is not essential, but simultaneous deletion of both genes results in late embryonic lethality.[7–9] However the lack of CDK6 results in defective proliferation of endocrine cells, anaemia, defects in T-cell development and anomalies in the haematopoietic system, which are not observed in CDK4 deficient cells, thereby inferring its functions differ from those of CDK4.[7–10] Indeed, over the past recent years several studies have revealed that CDK6 has cell-, tissue- and developmentally distinct functions from CDK4 and contributes to tumour development through different signalling pathways. Beyond its role in cell cycle coordination, CDK6 has been shown to exert functions in transcriptional regulation, tumour angiogenesis and metabolism.[11–17]

CDK6 links cell cycle progression to metabolism in cancer cells through phosphorylation of two key enzymes in the glycolytic pathway, 6-phosphofructokinase (PFKP) and pyruvate kinase M2 (PKM2), thereby inhibiting their catalytic activity.[17] CDK6 was shown to physically interact with the PFKP isoform of PFK1 and with PKM2 in five human T-ALL cell lines and its pro-survival function reported in tumours expressing high levels of CDK6-Cyclin D3.[17]

CDK6 overexpression and upregulation has been reported in several human cancers compared to noncancer cell lines in which it is expressed at low levels. In particular CDK6 is expressed at high levels in lymphoid malignancies in contrast to CDK4, more specifically in tumours which lack p16, in which CDK6 enhances proliferation and stimulates angiogenesis.[18] In hematopoietic malignancies such as AML and ALL, CDK6 has been reported to be involved in the transcriptional regulation of cancer-relevant genes such as VEGF-A and EGR1, FLT-3.[18] CDK6, but not CDK4, has been reported to promote transcription of $p16^{INK4A}$ through transactivation of c-JUN and STAT3, thereby contributing to its own controlled regulation in a negative feedback loop.[15] Furthermore, CDK6 contributes to early stages of tumorigenesis by binding to promoters of p53-antagonists and inducing a complex transcriptional programme that blocks p53-associated response in hematopoietic cells.[19] In melanoma, both CDK4 and CDK6 have been described to be required for tumour cell growth, proliferation and migration. Moreover there appears to be an interplay between these two kinases, the expression and availability of CDK4 defining the availability of CDK6 for transcriptional control of the angiogenic factor VEGF-A.[20] In lung adenocarcinoma tissues overexpression of nuclear CDK6 has been reported to play a detrimental role in disease progression and has been associated with poor

[a] J. Soamalala, S. Diot, Dr. M. Pellerano, Dr. M. C. Morris
Institut des Biomolécules Max Mousseron-IBMM-UMR 5247
Université de Montpellier, Faculté de Pharmacie
15, Av. Charles Flahault, 34093 Montpellier (France)
E-mail: may.morris@umontpellier.fr
[b] Dr. C. Blanquart
Université de Nantes, CNRS, INSERM, CRCINA
44000 Nantes (France)
[c] Dr. M. Galibert, Dr. M. Jullian, Dr. K. Puget
GENEPEP SAS
34430 Saint Jean de Védas (France)

Supporting information for this article is available on the WWW under https://doi.org/10.1002/cbic.202000677

overall survival rate and unfavourable prognosis in lung adenocarcinoma patients.[21] More recently CDK6 has also been reported to be coregulated with TRIM59 oncoprotein in lung cancer and the TRIM59-CDK6 axis most likely regulates growth and metastasis of lung cancer through activation of the ERK pathway.[22]

With the ever-growing evidence of CDK6 implication in cancer tumour formation and progression, it has become an established pharmacological target, together with CDK4.[14,23,24] However, despite its functional importance and oncological relevance, CDK6 has not been the subject of technological developments to probe and monitor its activity in a complex biological environment. To this aim we have developed a CDK6-specific fluorescent peptide biosensor (CDKACT6) that reports on CDK6 kinase activity through sensitive changes in fluorescence intensity. In this study we describe the design and characterisation of this biosensor derived from the CDK6 6-phosphofructokinase (PFKP) substrate reported by Wang et al.[17] We show that CDKACT6 biosensor can report on recombinant CDK6/cyclin D activity in dose-dependent fashion, and can be further applied to quantify differences in CDK6 kinase activity in melanoma and lung cancer cell extracts. We have further implemented CDKACT6 to characterise CDK6 activity in mesothelioma cell lines derived from patients, which were compared with CDK4 activities determined thanks to a CDK4-specific biosensor previously developed by our group.

Results and Discussion

Design and in vitro characterisation of a CDK6-specific peptide biosensor

Although CDK6 constitutes an established pharmacological target in cancer, no technologies have been developed to report on its kinase activity in a complex biological environment. In order to probe and monitor the relative activity of specific cell cycle kinases in a selective and sensitive fashion, we have developed a fluorescent biosensor technology and engineered several peptide biosensors that report on CDK4-specific and CDK5-specific activities.[25–27] These biosensors are synthetic modular polypeptides which combine a kinase-specific substrate moiety onto which an environmentally sensitive dye is conjugated, with a phosphoamino acid binding domain (PAABD), which specifically recognises the substrate when it is phosphorylated by the kinase of interest. Kinase activity and biosensor phosphorylation are monitored through changes in fluorescence, associated with the PAABD binding to the substrate moiety, which affects the local environment of the dye conjugated to the substrate moiety.

In order to engineer a CDK6-specific biosensor, we first designed peptide sequences derived from two recently identified substrates described to be phosphorylated by CDK6, pyruvate kinase M2 (PKM2) and phosphofructokinase P isoform (PFKP).[17] Specifically, peptide K6-1B was derived from PKM2 S37 phosphorylation site and two peptides K6-2A and K6-2D were derived from PFKP S679 phosphorylation site. To verify they were indeed recognised by CDK6, they were immobilised on CNBr-Sepharose and pulldown assays were performed with A375 cell extracts followed by western blotting with anti-CDK6 antibody (Figure 1A). Only K6-2D peptide retained CDK6 in A375 cell extracts. Since the PFKP substrate of CDK6 was initially identified in T-cell lines,[13] we performed pulldown experiments with immobilised K6-2D or Rb substrate peptide using Jurkat cell extracts to further address whether the K6-2D sequence was specific to CDK6 relative to its closely related homologue CDK4. Western blotting with anti-CDK4 and anti-CDK6 antibodies confirmed that CDK6 specifically bound the K6-2D peptide as well as the Rb substrate, whereas CDK4 was only retained by the Rb substrate (Figure 1B). To assess the affinity of this interaction we labelled K6-2D and Rb peptide with FITC and performed fluorescence titration experiments with recombinant GST-CDK4 and GST-CDK6 (Figure 1C). As a control we used a peptide substrate derived from the S795 phosphorylation site of p107Rb which is a recognised substrate of both

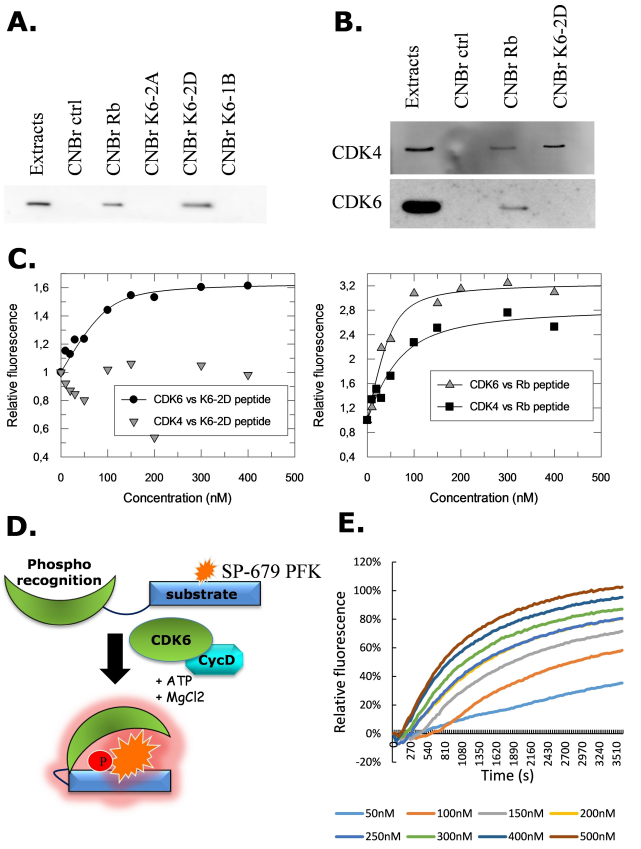

Figure 1. Design and characterisation of CDK6-specific peptide substrates. A) Pulldown experiments with Rb, K6-2A, K6-2D and K6-1B peptides immobilised on CNBr resins and incubated with cell extracts from A375 cells, followed by western blotting with anti-CDK6 antibodies. B) Pulldown experiments with Rb and K6-2D peptides immobilised on CNBr resins and incubated with cell extracts from Jurkat cells, followed by western blotting with anti-CDK4 and anti-CDK6 antibodies. C) Titration of 200 nM FITC-labelled substrates K6-2D and Rb peptides with recombinant CDK4 and CDK6 ($\lambda_{ex}=495$, $\lambda_{em}=520$ nm). D) Schematic representation of the CDKACT6 peptide biosensor. E) Dose-dependent response of 150 TAMRA-labelled CDKACT6 to recombinant CDK6 kinase: relative changes in fluorescence emission intensity over time biosensor incubated in PBS supplemented with 0.5 mM ATP, $MgCl_2$ ($\lambda_{ex}=535$, $\lambda_{ex}=585$ nm).

CDK4 and CDK6. Fluorescence emission of K6-2D remained unchanged upon titration with GST-CDK4 inferring it did not interact with recombinant CDK4.Titration experiments confirmed the pulldown experiments, revealing that CDK4 did not bind the K6-2D peptide. Curve fitting enabled calculation of a dissociation constant value of 11 ± 7.03 nM between K6-2D and GST-CDK6, and very similar values 9 ± 7.8 nM and 6.83 ± 7.5 nM for Rb binding to GST-CDK6 and GST-CDK4, respectively.

These studies revealed that K6-2D peptide was an appropriate and selective substrate of CDK6 over CDK4. We therefore designed a bipartite CDKACT6 biosensor comprising an N-terminal phospho-amino acid binding domain derived from the WW domain of Pin 1 (as described previously for CDKACT4 and CDKACT5 biosensors[25,27]) followed by the C-terminal K6-2D peptide substrate sequence, into which a TAMRA was incorporated on a lysine group at position −2 relative to the serine phosphorylation site (Figure 1D). We first addressed whether this fluorescent biosensor could respond to active recombinant CDK6/cyclin D1. To this aim we incubated 150 nM TAMRA-labelled CDKACT with different concentrations of recombinant CDK6 kinase between 50–500 nM and monitored changes in fluorescence emission intensity over time (Figure 1E and Figure S1 in the Supporting Information). These experiments revealed that CDKACT6 biosensor could effectively respond to CDK6 kinase activity in a dose-dependent fashion.

Application of CDKACT6 to probe CDK6 activity in cell extracts

To address whether CDKACT6 could be applied to monitor CDK6 activity in cell extracts and quantify relative differences in activity between different cell lines, we performed kinase activity assays using 150 nM TAMRA-labelled biosensor with 100 μg cell extracts derived from melanoma and lung cancer cell lines (Figure 2A). Specifically we compared CDK6 kinase activity in A375, A549, PC9 and H1299 cell extracts and found that A549 exhibited the greatest CDK6 activity, followed by A375, then PC9 and finally H1299. For comparison we used the TAMRA-labelled CDKACT4 biosensor we have previously developed[24] and monitored CDK4 activity in the same cell lines (Figure 2B). These studies revealed a very similar tendency, with CDK4 activity being the lowest in PC9 and H1299 lysates and greatest in A549 cell extracts. Comparison of the average relative fluorescence maxima corresponding to maximal response of each biosensor in these different cell lines is reported in Figure 2C and Table 1.

We further asked whether high kinase activity was necessarily associated with greater expression levels of either CDK4 or CDK6 in the different cancer cell lines. Western blotting revealed that both CDK6 and CDK4 protein levels were greater in A375 and H1299 cell lines (Figure 3A and B). We therefore calculated the specific activities for CDK4 and CDK6 kinases relative to their relative protein levels in each of these cell lines (Figure 3C, Table 2).Taken together this revealed a very high/important CDK6 kinase activity in the PC9 cell line, and a more

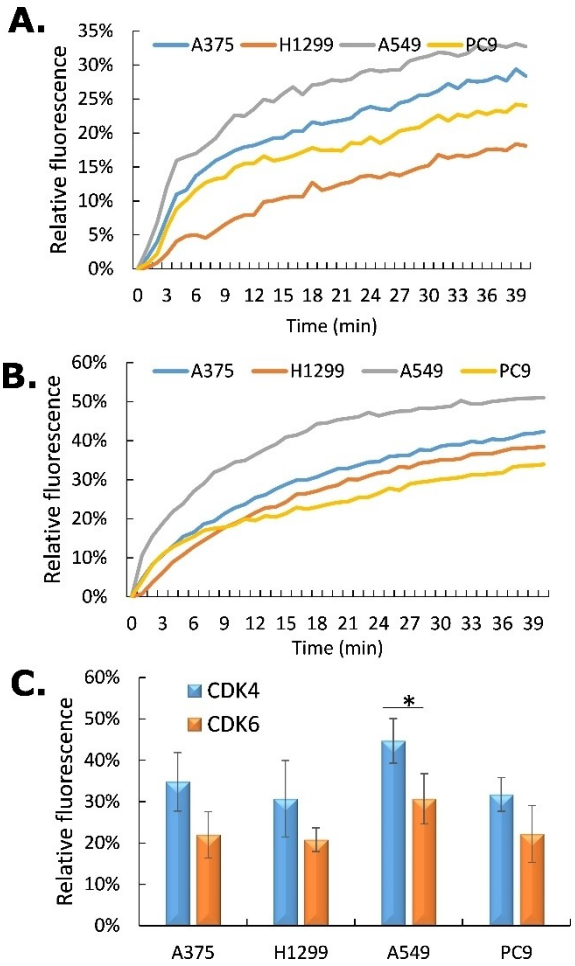

Figure 2. Application of CDKACT6 to report on CDK6 activity in cell extracts. A) Representative response of CDKACT6 biosensor to CDK6 activity in A375, A549, H1299 and PC9 cell extracts. B) Representative response of CDKACT4 biosensor to CDK4 activity in A375, A549, H1299 and PC9 cell extracts. C) Average CDKACT6 and CDKACT4 maximal response in A375, A549, H1299 and PC9 cell extracts (histogram values correspond to average timepoints at 2300s).

Table 1. Relative fluorescence maximum of CDKACT4 and CDKACT6 in different cell lines.

	Fluorescence maximum [%]	
	CDKACT4	CDKACT6
A549	45 ± 5	31 ± 6
H1299	31 ± 9	21 ± 3
A375	35 ± 7	22 ± 6
PC9	32 ± 4	22 ± 7

Table 2. Specific activity (relative activity/concentration) of CDK4 and CDK6 in different cell lines.

	Specific activity	
	CDKACT4	CDKACT6
A549	0.86 ± 0.10	1.58 ± 0.31
H1299	0.50 ± 0.15	0.29 ± 0.04
A375	0.35 ± 0.07	0.45 ± 0.12
PC9	1.10 ± 0.14	34.64 ± 11.02

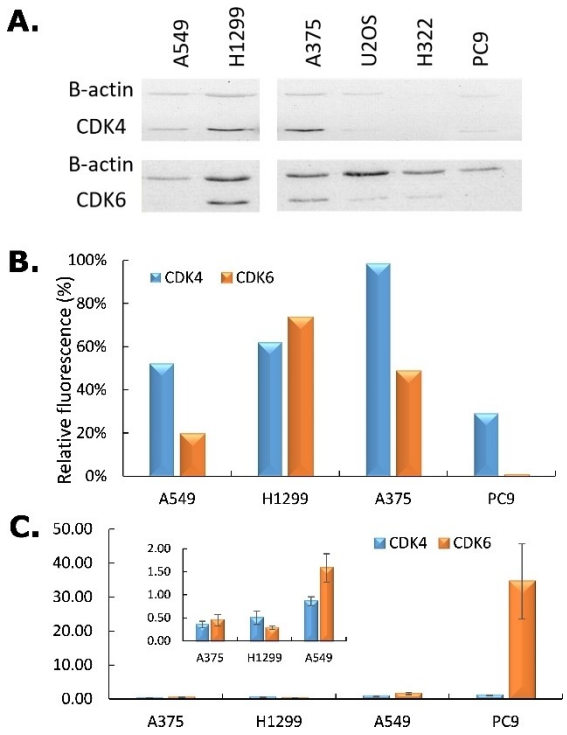

Figure 3. CDK4 and CDK6 specific activity in cell extracts. A) Western blot analysis of CDK6, CDK4 and actin levels in normalised A375, A549, H1299 and PC9 cell extracts. B) Quantification of CDK6 and CDK4 levels relative to actin. C) Specific activity of CDK6 and CDK4 (relative activity/relative concentration) in A375, A549, H1299 and PC9 cell extracts. The inset shows specific activities in A375, A549 and H1299 cell extracts.

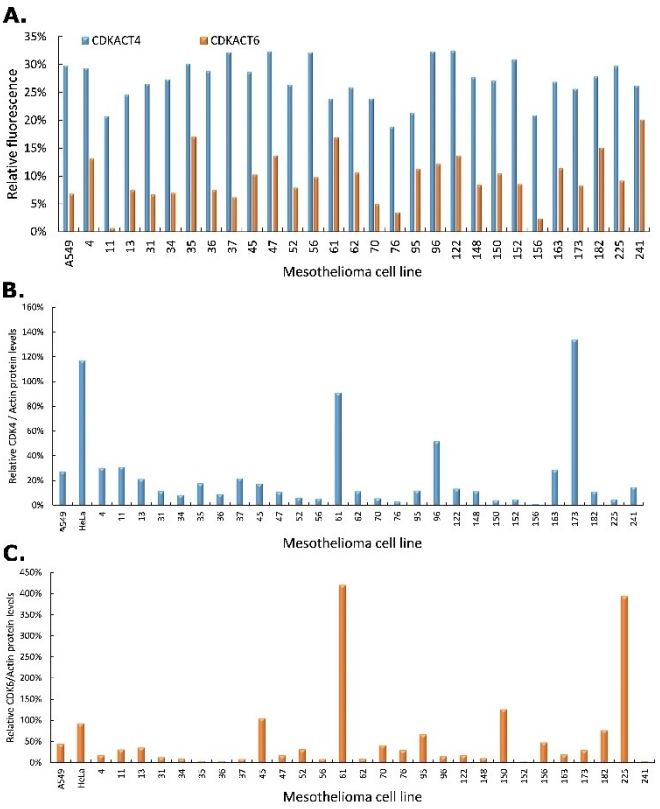

Figure 4. CDK6 and CDK4 activities in extracts from mesothelioma cell lines. A) Relative maximal activity of CDK4 and CDK6 determined with CDKACT4 and CDKACT6 biosensors, respectively, in different mesothelioma cell lines (after 2300s). Quantification of B) CDK4 and C) CDK6 levels relative to actin in normalised mesothelioma cell lines

modest yet higher CDK6 specific activity in A549 relative to the other cell lines.

Monitoring CDK6 and CDK4 relative activities in mesothelioma-derived cell extracts

In order to implement CDKACT6 biosensor to more complex samples, we asked whether any differences could be identified in lysates from a panel of mesothelioma cancer-derived cell lines (Figure 4A). Comparison of the relative fluorescence emission maxima in the different cell lines revealed important variations in CDK4 kinase activity but even more important differences in CDK6 activity. In certain cell lines such as Meso 11 and Meso 156, CDK6 was essentially inactive. In contrast CDK6 activity was the highest in samples 61 and 241. These studies enable clustering of cell lines with high CDK4 and CDK6 or low CDK4 and CDK6, or combinations of activities for either kinase.

Western blotting and quantification of CDK4 and CDK6 levels relative to actin revealed that there was no direct correlation between kinase activities and levels, thus implying the function of each of these kinase is regulated, dictated by other factors (Figure 4B and C)

Discussion

In this study we report a peptide biosensor comprising a short artificial phosphorecognition domain derived from the WW domain of Pin1 and a substrate sequence derived from PFKP onto which a TAMRA dye is conjugated, that responds to CDK6 activity through sensitive changes in fluorescence. Specifically, phosphorylation of the target serine prompts interactions between aromatic and positively charged residues in the PAABD (F, R, Y, R, W) and the negatively charged phosphoserine, thereby promoting folding of the PAABD onto the substrate sequence, as described previously.[25] As TAMRA is conjugated at position minus two relative to the phosphorylation site, these intramolecular conformational rearrangements significantly affect the polarity of its local environment and consequently its fluorescence emission.[29,30] Although there are no chemical linkers between the PAABD and the substrate moiety in this bipartite biosensor, the proline at the end of the artificial PAABD and the following serine and glycine residues ensure sufficient flexibility for the PAABD and the phosphorylated substrate moiety to interact. One of the most important criteria to be met in the design of a CDK6-specific biosensor is its selective response over CDK4, its most closely related kinase. By designing a new biosensor derived from a CDK6-specific

substrate through a rational approach, we have ensured it would not respond to CDK4 activity. Indeed, we have shown in pulldown assays that endogenous CDK4 does not bind the CDK6 substrate derived from PFKP whereas CDK6 does, and both kinases bind a peptide derived from the Rb substrate. It should be noted that in the design of the substrate moiety we replaced methionine at position 672 in the sequence of PFKP by sulfur-free and closely isosteric amino acid norleucine, with the aim of limiting oxidation issues.

The CDKACT6 biosensor was implemented to probe CDK6 kinase activity in a complex and physiologically relevant environment, total protein lysates derived from different melanoma and lung cancer cell lines which have been reported to harbour active CDK6. In fact we used both CDKACT6 and CDKACT4 biosensors to evaluate and compare the relative activities of CDK6 and CDK4 kinases respectively. Although the greatest response of both CDKACT6 and CDKACT4 biosensors was observed in A549 cell extracts, determination of specific activity, that is, activity relative to protein kinase expression revealed a very important CDK6 kinase activity in the PC9 cell line, and a more modest yet higher CDK6 specific activity in A549 relative to the other cell lines. Interestingly these two adenocarcinoma cell lines differ notably in their p53, EGFR and KRAS status, A549 expressing wildtype p53, wild-type EGFR and KRAS mutant, whereas PC9 expresses the R248Q mutant form of p53 and mutant EGFR.

Moreover, we have characterised CDK4 and CDK6 kinase activity and expression levels in different mesothelioma cell lines derived from patients and found very different activity patterns throughout cell lines. Our work therefore demonstrates that the CDK6 and CDK4 peptide biosensors constitute selective tools for monitoring these two closely relative kinases in parallel. Interestingly, several recent studies have reported therapeutic perspectives for treatment of mesothelioma using CDK4/6 inhibitors and Palbociclib appears to reduce phosphorylation of CDK6 and Rb.[28] As CDK6 also appears to be upregulated in lung cancers more generally and plays an important role in cancer cell survival,[17,20–22] the CDK6 biosensor described in this study and its combination with the previously reported CDK4 biosensor could provide important information to guide therapeutic intervention.

Taken together these results reveal that the CDKACT6 peptide biosensor constitutes a specific and sensitive tool to assess the relative activity of CDK6 using cell extracts as a source of kinase. Furthermore this original technology can be implemented to probe CDK6 hyperactivity in pathological samples and to distinguish the specific inhibition of this kinase by therapies that target both CDK4 and CDK6.

Experimental Section

Peptide synthesis and purification: Peptide K6-1B was derived from Pyruvate Kinase M2 (PKM2 S37 phosphorylation site) in which a unique lysine was introduced at position −2 relative to the phosphorylation site. Peptides K6-2A and K6-2D were derived from Phospho Fructo Kinase P isoform (PFKP S679 phosphorylation site). Peptide K6-2D is a shorter variant of K6-2A, in which the oxidisable methionine was replaced with the sulfur-free and closely isosteric amino acid norleucine, and a unique lysine was introduced at position −2 relative to the phosphorylation site, replacing the alanine in K6-2A and the endogenous sequence of PFKP.

CDKACT6 biosensor was designed to combine a sequence derived from the WW domain of Pin 1 (sequence GFARVYMSRSSGWERPSGG) with substrate sequence K6-2D. A TAMRA labelled lysine residue was introduced at position −2 relative to the serine phosphorylation site. CDKACT4 biosensor has been described previously.[25]

Synthesis-grade Fmoc-AA reagents and HATU were purchased from Iris Biotech. FITC, Rink amide resin (200–400 mesh, 0.34 mmol/g) DMF, DCM, methanol, diethyl Et_2O, and HPLC-grade acetonitrile were purchased from Aldrich TAMRA alkyne (CAS N°: 945928-17-6) and TAMRA maleimide was purchased from Lumiprobe GmbH.

All peptides were synthesised at the 100 μmol scale using Fmoc-SPPS on a Symphony X instrument (Protein Technologies, Inc., USA).The standard deprotection-coupling cycle for each residue consisted of six steps: The resin was washed with 5 mL DMF (3× 30 s). The Fmoc group was deprotected with 5 mL 20% piperidine in DMF (3×3 min). The resin was washed with 5 mL DMF (3×30 s). Fmoc-AA was coupled for 60 min using HATU and iPr_2NEt as coupling agent. At the end of the coupling cycle, a capping step was performed with 5 mL 10% Ac_2O in DMF for 7 min and the resin was extensively washed with 5 mL DMF (3×30 s). Once finished, peptide resins were washed three times with both DMF and DCM and then cleaved with TFA cleavage cocktails (per 100 μmol scale synthesis): 17.5 mL TFA, 500 μL TIS, 500 mg Phenol, 1000 μL water, 500 μL Ethanedithiol and 500 μL tetrabutylammonium bromide. After 3 h, the cleavage solution was filtered from the resin, and peptides were precipitated from Et_2O. The resulting precipitated peptides were centrifuged at 4000 rcf, and the supernatants were decanted. Peptides were washed twice more with ether, and then dried for >3 h in vacuum desiccator prior to dissolution, analytical characterisation, and purification.

Peptides were analysed by UPLC and ESI-MS mass spectrometry. Instruments were equipped with BEH C18 (WATERS), 150×2.1 mm (150×2.1 mm flow rate: 0.6 mL/min). Solvents A and B were 0.1% TFA in water and 0.1% TFA in acetonitrile. Specific details concerning synthesis and purification of each peptide are described in the Supporting Information.

K6-1B: RLDKD**SP**PITARNTG

K6-2A: VLGHMQQGGAP**SP**FDRNFGT

K6-2D: GH£QQGGKP**SP**FDRNFG

CDKACT4: GFARVYMSRSSGWERPSGG YKFCSSPLRIPG

CDKACT6: GFARVYMSRSSGWERPSGG GH£QQGGKP**SP**FDRNFGT

£: norleucine

Rb peptide substrate (YKFCSSPLRIPG) was derived from S795 of p107 Retinoblastoma protein. It was synthesised by GLS Peptide and purified to 95% purity by HPLC.

For titration experiments with recombinant CDKs, Rb peptide was labelled on the single cysteine residue with FITC, in the presence of a five- to tenfold excess of dye overnight, and then purified from free dye on NAP-5 columns (GE Healthcare). K6-2D was labelled with FITC on the internal lysine as described in the Supporting Information.

Protein expression and purification. Recombinant GST-CDK6, GST-CDK4 and GST-cyclin D were expressed in *E. coli* (BL21 DEA3) overnight at 20 °C following induction with 1 mM isopropyl β-D-1-thiogalactopyranoside (IPTG). The soluble protein fraction of GST-

CDK6 was then purified by FPLC on a GSTrap HP 5 mL column (GE Healthcare) equilibrated in buffer A (50 mM Tris, pH 7.4, 250 mM NaCl). The soluble protein fraction of GST-CDK4 was purified by FPLC on a GSTrap HP 5 mL column (GE Healthcare) equilibrated in buffer B (50 mM phosphate, pH 6.4, 500 mM NaCl). The soluble protein fraction of GST-Cyclin D1 was purified by FPLC on a GSTrap HP 5 mL column (GE Healthcare) equilibrated in buffer C (50 mM Phosphate, pH 7.4, 150 mM NaCl). GST-tagged proteins were eluted with buffer A, B or C containing glutathione (50 mM Euromedex), and then further purified on desalting columns (GE Healthcare) in their corresponding buffer.

Fluorescence titration experiments. Fluorescence titration assays were performed in 96-well plates in a thermostated chamber (Clariostar spectrofluorimeter, BMG) at 30 °C in 200 µL phosphate buffer saline (PBS) purchased from Sigma. 200 nM FITC-labelled peptides were excited at $\lambda = 483$ nm, and emission signals were acquired at $\lambda = 530$ nm.

Curve fitting and determination of dissociation constants were performed with the GraFit 7 software (Erithacus, Ltd., Horley, UK) using the following quadratic equation:

$$F = F_{min} + (F_{max} - F_{min}) \times \frac{K_d + L + p - \sqrt{(K_d + L + p)^2 - 4p}}{2p}$$

In which L is the concentration of ligand and p is the concentration of fluorescent peptide biosensor.

Fluorescence kinase activity assays. Fluorescence kinase activity assays were performed essentially as described previously[25–27] at 30 °C in a thermostated chamber (Clariostar spectrofluorimeter, BMG) in 96-well plates 200 µL phosphate buffer saline (PBS, Sigma), supplemented with 5 mM $MgCl_2$, 0.5 mM ATP. Changes in fluorescence emission of TAMRA-labelled peptide biosensors were recorded at 585 nm following excitation at 535 nm. In all experiments, relative fluorescence was calculated following subtraction of biosensor fluorescence from fluorescence values obtained in the presence of protein kinases or cell extracts. Data analysis was performed using the GraFit 7 Software (Erathicus Ltd). Experiments were performed in triplicate, and error bars indicate standard deviation from average. Histograms represent relative fluorescence intensity values after 2300s, unless specified otherwise.

Cell culture and extract preparation. Jurkat, A549, H1299 and PC9 cell lines were cultured in RPMI (Life Technologies) and A375 in DMEM + Glutamax (Invitrogen) supplemented with 10% FCS and antibiotics (100 units/mL penicillin (G sodium salt) and 100 µg/mL streptomycin) at 37 °C in an atmosphere containing 5% CO_2. Cell extracts were prepared in PBS lysis buffer (PBS Sigma, 0.2% NP40) complemented with 1 mM EDTA, 2 mM PMSF, Complete™ protease inhibitors (Roche), and total protein concentration was normalised by spectrophotometric dosage at 280 nm.

Mesothelioma cell lines. Mesothelioma cell lines were established from pleural effusions aseptically collected from patients with a suspicion of mesothelioma, prior to anticancer therapy, by thoracocentesis at the Laënnec Hospital (St-Herblain, France).[31] Diagnoses were established, using both fluid cytology and immunohistochemical staining of pleural biopsies, by the pathology department at Laënnec Hospital and then externally confirmed by MESOPATH, a network of French pathology experts for the diagnosis of mesothelioma. All recruited patients have given signed informed consent. All the collected samples and the clinical information belong to a biocollection (DC-2011-1399) validated by the French Ministry of Research. All cell lines were cultured at 37 °C under 5% CO_2 in RPMI-1640 medium (Gibco) supplemented with 2 mM L-glutamine, 100 IU/mL penicillin, 0.1 mg/mL streptomycin and 10% heat-inactivated foetal calf serum (FCS Gibco).

Pulldown experiments and western Blotting. Peptides were coupled onto CNBr Sepharose resin ($10^{<M->3}$M peptide per g resin GE Healthcare) and incubated with 1 mg cell extracts for 1 h at 4 °C, then washed twice with PBS. The resin was boiled in Laemmli buffer and proteins retained on the resin were separated by SDS-PAGE, then transferred onto PVDF membranes (Immobilon-P, Merck Millipore) for 2 h at 100 V using a liquid BioRad system. Western blotting was performed according to standard procedures: membranes were first saturated with 5% milk in PBS, 0.1% Tween, then incubated overnight at 4 °C with the monoclonal rabbit anti-CDK6 antibody (Cell Signaling D4S8S, #13331), anti CDK4 antibody (Cell Signaling D9G3E, #12790) or polyclonal rabbit β-actin antibody (Cell Signaling, #4967) diluted 1:500 (anti-CDK6) or 1:1000 (anti-CDK4 and β-actin) in PBS 0.1% Tween. Membranes were then washed three times for 10 min with PBS 0.1% Tween and incubated for 1 h at room temperature with horseradish peroxidase-conjugated secondary antibodies (GE Healthcare, #NA934 V) diluted 1:10000 in PBS 0.1% Tween. After three final 5 min washes with PBS 0.1% Tween, membranes were processed with ECL prime (GE Healthcare, #RPN2232) and signals were detected with an Amersham Imager 680 from GE Healthcare. Quantification of signals was performed using Image J.

Statistics. The Wilcoxon unpaired method was used and all p values were calculated on Rstudio by using the "wilcox.test" function. All interactions were performed 3 times and activity assays 4 times. P values * $p \leq 0.05$, ** $p \leq 0.01$, *** $p \leq 0.001$

Acknowledgments

This work was supported by the CNRS (Centre National de la Recherche Scientifique) and a grant from the French Region Occitanie and the European Regional Development Fund (READY-NOV/FEDER no. 2018-003539-01) to M.C.M. and K.P.

Conflict of Interest

The authors declare no conflict of interest.

Keywords: CDK4 · CDK6 · fluorescent biosensors · kinases · lung cancer · mesothelioma · peptides

[1] Matsushime, H. Ewen, M. E. Strom, D. K. Kato, J. Y. Hanks, S. K. Roussel, M. F. Sherr, *J. Cell* **1992**, *71*, 323–34.
[2] Meyerson, M. Harlow, *E. Mol. Cell. Biol.* **1994**, *14*, 2077–2086.
[3] Bates, S. Bonetta, L. MacAllan, D. Parry, D. Holder, A. Dickson, C. Peters, *Oncogene* **1994**, *9*, 71–79.
[4] A. S. Lundberg, R. A Weinberg, *Mol. Cell. Biol.* **1998**, *18*, 753–761.
[5] J. W. Harbour, R. X. Luo, A. Dei Santi, A. A Dean Postigo, *Cell* **1999**, *98*, 859–869.
[6] S. M. Rubin *Biochem Sci.* **2013**, *38*, 12–9.
[7] Malumbres M. Sotillo, R. Santamaría, D. Galán, J. Cerezo, A. Ortega, S. Dubus, P. Barbacid, *Cell* **2004**, *118*, 493–504.
[8] P. Kozar, K. Sicinski, *Cell Cycle* **2005**, *4*, 388–391.
[9] C J Sherr, J M. Roberts, *Genes Dev.* **2004**, *18*, 2699–711.
[10] Hu, M. G. Deshpande, A. Enos, M. Mao, D. Hinds, E. A. Hu, G. F. Chang, R. Guo, Z. Dose, M. Mao, *Cancer Res.* **2009**, *69*, 810–818.
[11] S Lim, P Kaldis, *Development.* **2013**,*140*, 3079–93.
[12] P Hydbring, M Malumbres, P Sicinski, *Nat Rev Mol Cell Biol.* **2016** *17*, 280–92.

[13] Tigan A. S. Bellutti, F. Kollmann, K. Tebb, G. Sexl, *Oncogene* **2016**, *35*, 3083–3091.
[14] Tadesse, S. Yu, M. Kumarasiri, M. Le, B. T. Wang, *Cell Cycle* **2015**, *14*, 3220–3230.
[15] Kollmann, K. Heller, G. Schneckenleithner, C. Warsch, W. Scheicher, R. Ott, R. G. Schäfer, M. Fajmann, S. Schlederer, M. Schiefer, *Cancer Cell* **2013**, *24*, 167–181.
[16] Scheicher, R. Hoelbl-Kovacic, A. Bellutti, F. Tigan, A. S. Prchal-Murphy, M. Heller, G. Schneckenleithner, C. Salazar-Roa, M. Zöchbauer-Müller, S. Zuber, *Blood* **2015**, *125*, 90–101.
[17] Wang, H. Nicolay, B. N. Chick, J. M. Gao, X. Geng, Y. Ren, H. Gao, H. Yang, G. Williams, J. A. Suski, *Nature* **2017**, *546*, 426–430.
[18] J Chen, M. M. Chiu, S. C. Chen, K. C. Huang, Y. R. J. Liao, Y. T. A. Yu, C. T. R. Oncol , *Lett.* **2020**, *19*, 3189–3196.
[19] F. Bellutti, A.-S. Tigan, S. Nebenfuehr, M. Dolezal, M. Zojer, R. Grausenburger, S. Hartenberger, S. Kollmann, E. Doma, M. Prchal-Murphy, et al., *Cancer Discovery* **2018**, *8*, 884–897.
[20] Kollmann, K. Briand, C. Bellutti, F. Schicher, N. Blunder, S. Zojer, M. Hoeller, *Oncotarget* **2019**, *10*, 1346–1359.
[21] L H. Zhang, J. Xie, *Int. J. Clin. Exp. Pathol.* **2017**, *10*, 9614–9620.
[22] G B. Liang, M. Qin, L. Zhao, W. Wang, H. Wang, L. Pan, X. Chen, *J. Cell. Mol. Med.* **2019**, *23*, 1458–1469.
[23] C. J. Sherr, D. Beach, G. I. Shapiro, *Cancer Discovery* **2016**, *6*, 353–67.
[24] G S. DeCristo, M. J. McAllister, S. S. Zhao, *Trends Cell Biol.* **2018** *28*, 911–925.
[25] Prével, C. Pellerano, M. González-Vera, J. A. Henri, P. Meunier, L. Vollaire, J. Josserand, V. Morris, *Biosens. Bioelectron.* **2016**, *85*, 371–380.
[26] V T. N. h. N. Pellerano, M. Lykaso, S. Morris, *ChemBioChem* **2014**, *15*, 2298–2305.
[27] M. L. Peyressatre, A. Pellerano, M. Boukhaddaoui, H. Soussi, I. Morris, *Biotechnol. J.* **2020**, e1900474.
[28] M. A. Bonelli, D G. Fumarola, C. Alfieri, R. Quaini, F. Falco, A. Madeddu, D. La Monica, S. Cretella, D. Ravelli, *Neoplasia* **2017**, *19*, 637–648.
[29] D. A. Hinckley, P. G. Seybold Borris, *Spectrochimica Acta* **1986**, *42*, 747–754.
[30] S. Galen, M. S. Loving, B. Imperiali, *Trends Biotechnol.* **2011**, *28*, 73.
[31] F. Gueugnon, S. Leclercq, C. Blanquart, C. Sagan, L. Cellerin, M. Padieu, C. Perigaud, A. Scherpereel, M. Gregoire, *Am. J. Pathol.* **2011**, *178*, 1033–1042.

Manuscript received: September 29, 2020
Revised manuscript received: October 26, 2020
Accepted manuscript online: October 28, 2020
Version of record online: ■■, ■■■

FULL PAPERS

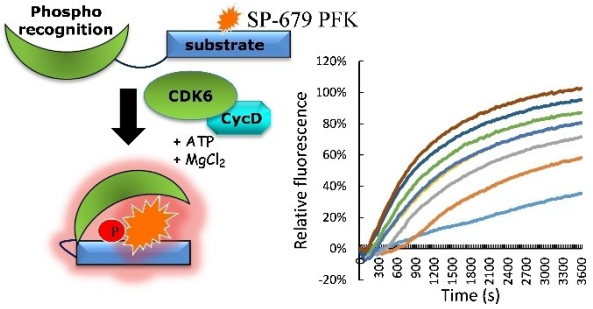

*J. Soamalala, S. Diot, Dr. M. Pellerano, Dr. C. Blanquart, Dr. M. Galibert, Dr. M. Jullian, Dr. K. Puget, Dr. M. C. Morris**

Distinguished kinases: We describe the design, engineering and characterisation of a fluorescent peptide biosensor derived from 6-phosphofructokinase, that reports on CDK6 kinase activity in vitro and in lung cancer cell extracts. Implementation of this biosensor in mesothelioma cell lines derived from patients highlights differences between CDK6 kinase activity and closely related CDK4 kinase activity.